EasyChair Preprint

№ 9140

Modeling and Analysis of 12/8 Switched Reluctance Machine by Finite Element Method with Taking into Account No-Linearity Effects

Zine Mahmoud, Labiod Chouaib, Srairi Kamel, Remha Souheib, Benbouzid Mohamed and Boughezalah Mohamed Salah

October 26, 2022

Modeling and analysis of 12/8 Switched Reluctance Machine by Finite element method with taking into account no-linearity effects

M. Zine[a], C. Labiod[b,c], K. Srairi[c], S. Remha[d], M. E. H. Benbouzid, S. Boughazala Mohamed[e]

[a]*LEVRES—Research Laboratory, Dept. of Electrical Engineering, University of El Oued, B.P.789, 39000 El Oued, Algeria*.
[b]*Faculty of technology, University of El Oued, B.P.789, 39000 El Oued, Algeria.*
[c]*Laboratory of Energy Systems Modeling (LMSE), Department of Electrical Engineering, University of Biskra, BP 145, 07000 Biskra, Algeria.*
[d] *Department of Electrical Engineering, LACoSERE Laboratory, Amar Thelidji University, BP 37G road of Ghardaia, Laghouat, Algeria*
[e]*University of Brest, UMR, CNRS 6027 IRDL.*

Abstract

This paper deals with analysis of the non-linear effects on the 12/8 switched reluctance machine. The characteristics curve has a high nonlinear magnetic circuits and nonlinear geometric, where the air gap varied according to the rotation mode. Therefore, the finite element method is a powerful tool for modeling and resolving this non-linear problem. In this paper, two cases for the magnetic characteristic, one by taken a numerous linear state of the permeability from the non-linear curve B = f (H) and the second position by looking all the nonlinear curve B = f (H). The static characteristics of the SRM are modeled by two-dimensional finite element with different rotor positions as electric current (excitation) changes. Analyze the results of the two cases based on the comparative study results. The obtained results demonstrate the importance of the nonlinear recognition in SRM. In order to evaluate these features, the finite element modeling process is presented in two cases, one by considering only the non-linearity of the geometry (air gap variance) and the second one by considering the nonlinear properties of the components (nonlinear magnetic circuits) with nonlinear geometries.

Keywords: Switched reluctance motor, Inductance characteristics, Non-linearity, Magnetic circuit, Numerical modeling, Finite elements method.

1. INTRODUCTION

We have conducted studies on the characteristics of the frequency start machine, the features of the latter are reflected in several advantages, that draw attention to focus more and more on the it. The advantages of SRM can be presented in a simple structure, low cost, durability, rotor, absence of permanent magnets, non-winding construction in one side, continuity of service in case of failure and ability to use in high temperature environments or during strong temperature changes[1,2].However, there are some shortcomings of the machine such as sound noise due to fluctuations in speed and high ripples of torque, and it is characterized by nonlinear characteristics due to magnetic saturation SRM, dual prominent structure, and difficulties in control, modeling and analysis[1-3].

The finite element method was first introduced in the field of structural analysis, as it was introduced from the methods of the scientist Courant in 1943 and was not exploited until 1968 on electromagnetic problems .With continuous research and application of mathematical algorithms to solve many electromagnetic problems. Therefore, the finite element method (FEM) has aroused great interest from researchers in many studies and has been used as a design and analysis tool in many fields of applied engineering such as machinery. rotating, computational fluid mechanics, etc [4,5].

Researchers are interested in using the finite element method to solve many physiological and electromagnetic problems [6]. Other authors have published works, in which the operating theory of the SRM is presented The theoretical methods adopted and the numerical modeling performed to compare results mainly, in terms of complexity in computation problems especially in regions of heterogeneity, air gap and for more accurate results[7].

The nonlinear height and complexity of the analysis and estimation of SRM characteristics have been discussed in several articles.[8-10].However, two stages of nonlinear computation have to be emphasized in the SRM. To this end, we worked by FEM to model and analyze a nonlinear model of 12/8 SRM to identify the various properties and geometric behavior of the SRM. Moreover, we compared the obtained results from the nonlinear model with the one of the linear model in order to find out the difference between the two models, the extent of nonlinearity inherent in the SRM and the available range for linear use.

2. DESIGN AND MODELING OF SRM BY FEM

We will use the two-dimensional FEM in electrical machine simulation, where this latter is usually simpler and quicker than the three-dimensional FEM, because of the symmetry of the electrical machine, there is a strong consistency between the 2D and 3D results. The geometry of the unit must be extended to the measurement of inductance, flux and other static parameters with FEM. The machine engineering parameters are shown in the Table I [6],[10].

The definition of magnetic permeability for each area according to the properties of the material or space is required for electromagnetic modeling by the FEM. For the rotor yoke and the stator, the magnetization curve of the material is presented in Fig. 1.

Thanks to the curve B-H as indicated in fig.1, we define the magnetic material in the nonlinear state, where the effects of magnetic saturation are counted in order to obtain static characteristics based on the use of finite element modeling.

Table I. The SRM dimensions.

SRM Ns/Nr		12/8
Polar arc of the stator βs	[Deg]	15.18
Polar arc of the rotor βr	[Deg]	15.23
stator outer radius	[mm]	89.8
Inside radius of stator cylinder head	[mm]	78.4
Inside radius of stator	[mm]	48.18
Rotor outer radius	[mm]	47.82
Rotor cylinder head outer radius	[mm]	30.3
Shaft radius	[mm]	15
Active length	[mm]	165
Number of series turns/phase		55

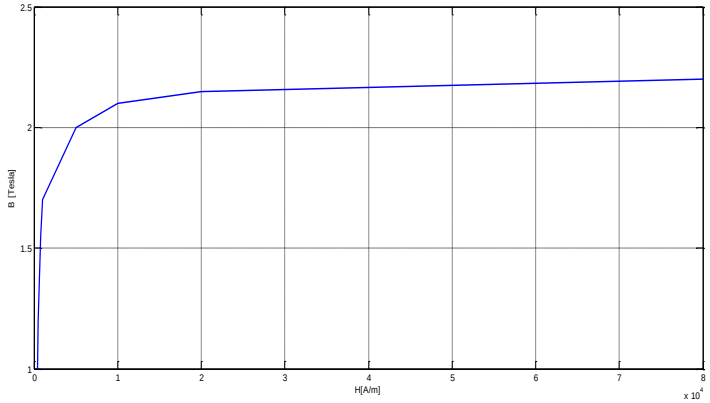

Fig. 1. Magnetization curve for the SRM yoke.

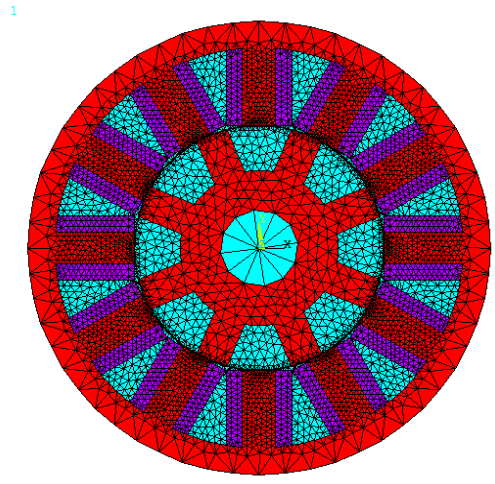

Fig. 2. Mesh discretization on the 12/8 SRM.

Using the geometric parameters from the previous table 1, we design a 12/8 SRM in the ansys software as shown in figure 2. In order to measure the total electromagnetic quantities, the size of the elements is very important. More accurate results and longer calculation time are provided by smaller components, and vice versa. Note that the technical grids used in this model are as follows: at

the level of the air gap, the large elements within the boundaries of the machine get smaller, smaller as the line slides further and further into the center of the SRM

The technical grid used in Figure 2 achieves accurate results using arithmetic time, and in areas where the differences in the values of the results are large, we use the smaller elements. In areas, where these differences are not significant, the most important elements are adopted. During our study of linear or nonlinear cases, we will use this economic and technical choice of component distribution model during modeling. This selection guarantees very good quality and important results.

In reference [6],[10-12] The necessity of employing the FEM to obtain the magnetic characteristic in SRM was confirmed by the authors. However, because to SRM's unique shape, several exact calculation issues have arisen, particularly in the air gap and heterogeneity zones. As a result, various studies have been conducted in recent years to adjust the MEF with SRM in order to obtain more accurate results.

The magnetic distribution will acquire the value of the magnetic vector voltage $\vec{A}$ allowed by it and the properties of the nonlinear magnetic material.

Poisson's equation is defined as follows:

$$curl\left(v\ curl\vec{A}\right) = \vec{j} \tag{1}$$

where ν is the magnetic reluctivity and J_z the source current density:

$$\frac{\partial}{\partial x}\left(v\frac{dA_z}{dx}\right) + \frac{\partial}{\partial y}\left(v\frac{dA_z}{dy}\right) = -J_z \tag{2}$$

Access to the value of the flux linkage for one-step in SRM can be dependent on the outcome of the magnetic vector potential A.

$$\emptyset = \frac{1}{i}\int_{v}^{\cdot} \bar{J}\bar{A}dV \tag{3}$$

After determining the specific elements with respect to the axial length of the machine

Equation (2) is the number of turns per phase N, and the winding area of phase S becomes:

$$\emptyset = \frac{NI}{S}\sum_{k=1}^{N} A_k\, S_k \tag{4}$$

The inductance and the magnetic co-energy are calculated according to the following formula as a function of the flux linkage:

$$L(\theta, i) = \frac{\emptyset(\theta, i)}{i} \tag{5}$$

$$W_{em} = \int_{0}^{\grave{\iota}} \emptyset(\theta, \iota)\, \partial i|_{\theta=const} \tag{6}$$

The torque is determined by the derivative of the magnetic energy of common angular position as shown in the following equation:

$$T(\theta, i) = \frac{\partial \grave{W_{em}}}{\partial \theta}|_{i=const} \tag{7}$$

Due to its ability and compatibility to perform modeling for all specifications and to achieve the necessary properties, the SRM 12/8 model for linear and nonlinear cases was implemented and evaluated using the ANSYS APDL language.

In this section, in the case of the magnetic model, we will introduce the FEM-based SRM. The static magnetic model, the first step that relies on the analysis of electromagnetic behavior, the transmittance will be calculated based on the curve B=f(H) (see Figure

5). Its use in the case is linear with change of rotation position and the second case is nonlinear. In the second case, the external circuit current values can differ as a function of the different angular locations of the rotor. In order to find out the static features in the linear and nonlinear state of the magnetic circuit, place them on the misalignment position.

3. GRAPHICAL ANALYSIS RESULTS

The structure and geometry of SRM 12/8 are symmetric and homogeneous, allowing only one phase to be identified and analyzed to obtain properties of other phases.

To acquire the characteristics of the SRM, we can model the system from an unaligned site with varying electric currents to assess the nonlinear FEM and model the system from the variable transmittance from to evaluate the linear FEM. After modeling by FEM, the simulation results for the two cases can be seen and the results are compared.

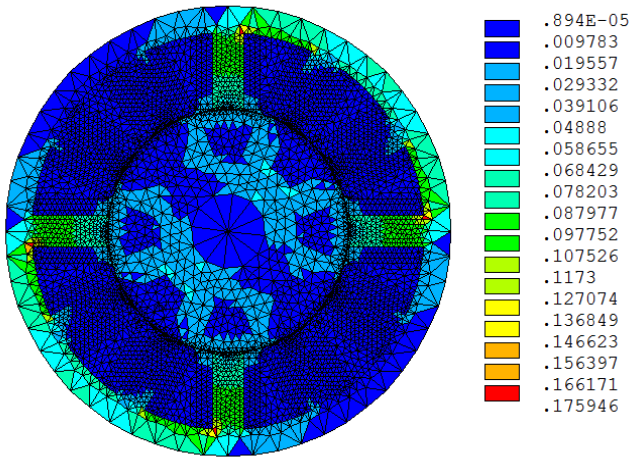

μ =1541.36

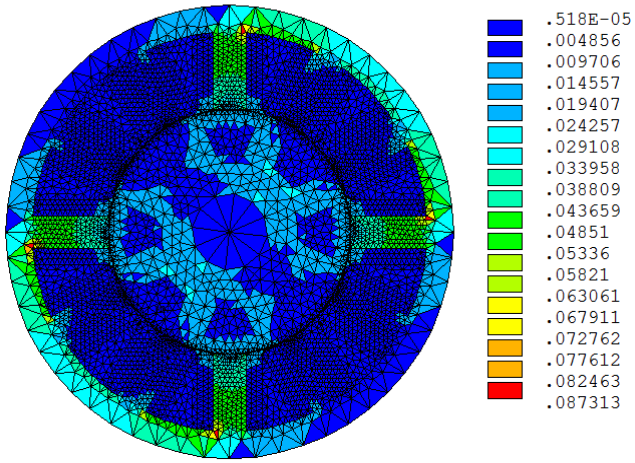

μ =1352.42

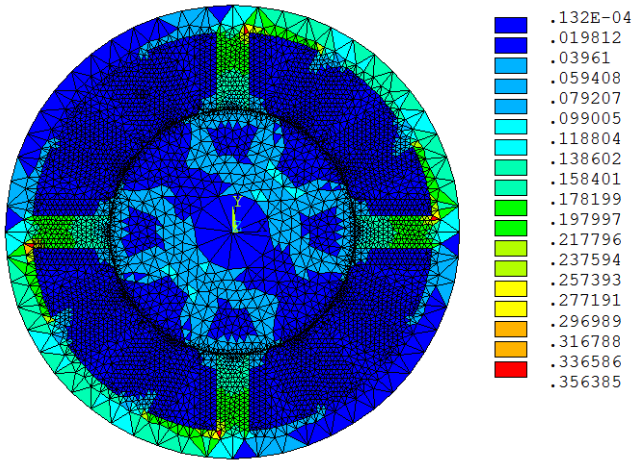

μ =1988.86

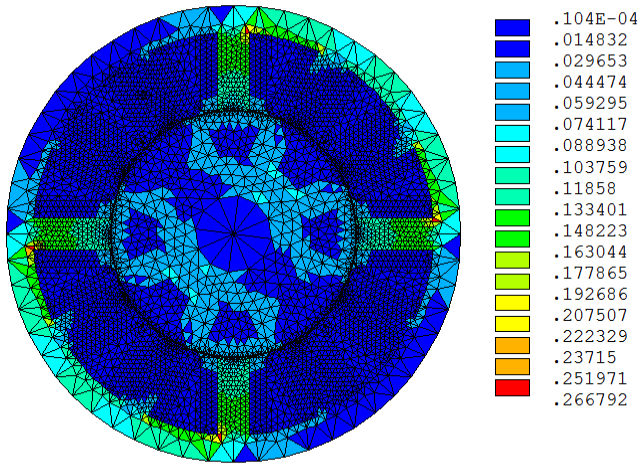

μ =1909.3

Fig.3 . The flux density is a variable function of the permeability of the linear case.

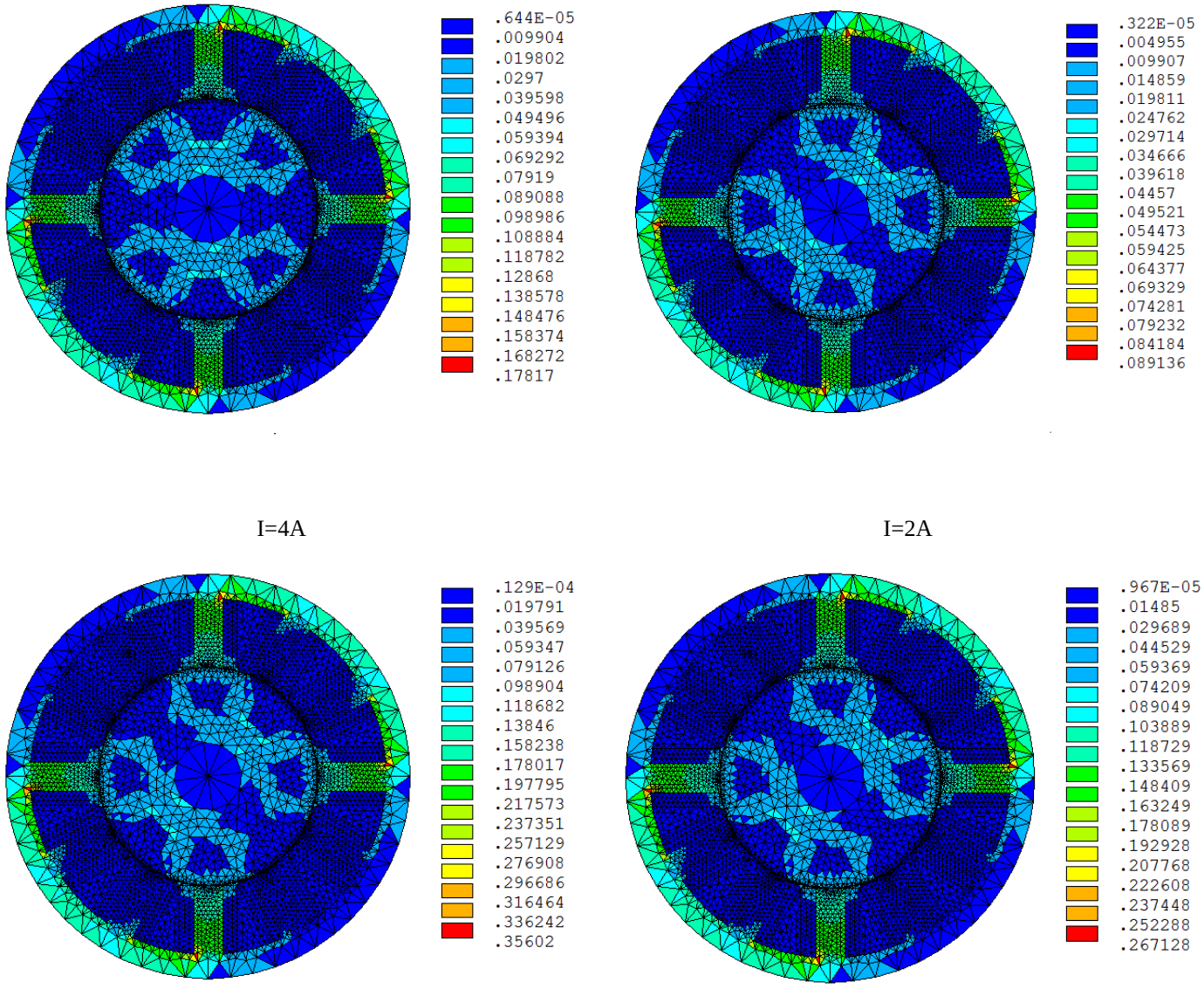

Fig. 4. The flux density is a variable function of the excitation current of the non-linear case.

Figure 3 and Figure 4 show the magnetic flux density, obtained from the two extreme positions of linear and nonlinear states. In Fig. 3 the flux density is a variable function of linear state permeability, and we note that the symmetric distribution of magnetism increases the flux density according to the magnetic curve B =f(H) (See Figure 1) for the B=f(H) curve. We calculate the permeability values in the pre-saturation region (for the non linear case), the saturation region, the air gap displacement and the magnetic circuit.

In Figure 3, the mean values obtained range from 0.043 to 0.058 Tesla and the maximum values at the angles of the magnetic circuit are up to 0.087 Tesla for permeability $\mu = 1352.4$. And between 0.117 and 0.087Tesla, the maximum values at the angles of the magnetic circuit reach 0.175 Tesla for permeability $\mu = 1541.36$, and between 0.133 and 0.177 Tesla, and the maximum values at the angles of the magnetic circuit reach 0.266 Tesla for permeability $\mu = 1909.3$, and between 0.178 and 0.237 Tesla and the maximum values are reached At angles of the magnetic circuit to 0.356 Tesla for permeability $\mu = 1988.86$.

However, in Fig4, the magnetic flux density was obtained as a function of a current change of the nonlinear state. We note that the extreme positions and increments, the magnetic flux density distribution is the same. Magnetic induction value without linear saturation. The mean values obtained here range from 0.044 to 0.059 Tesla and the maximum values at angles of the magnetic circuit are up to 0.089 Tesla for transmittance I = 2A. And between 0.118 and 0.089 Tesla, the maximum values at the angles of the magnetic circuit reach 0.178 Tesla for transmittance I = 4A, and between 0.133 and 0.178 Tesla, and the maximum values at the angles of the magnetic circuit reach 0.267 Tesla for transmittance I = 6A and between 0.178 and 0.237 Tesla has been reached. Maximum values at angles of magnetic circuit to 0.356 Tesla for transmittance I=8A.

We notice from Fig. 3 and Fig. 4 that the flux density is equal for linear and nonlinear states. The permeability μ= 1352.42 for linear state equal to the current I = 2A.For nonlinear state, the permeability μ = 1541.42 for the linear state and the current is equal to I = 4A.For the nonlinear state, the permeability μ = 1909.3 for the linear state the current is equal to I = 6A.For the nonlinear state, the permeability μ = 1988.86 for the linear state the current is equal to I = 8A for the nonlinear state.

4. CURVES NETWORK ANALYSIS

Judging from the previous relationships (Eq. (4), Eq. (5) and Eq. (6)) allow to calculate magnetic field strength, inductance, magnetic flux density, constant torque, and flux correlation, to solve the Eq. (6) to determine the voltage of the magnetic vector.

The important properties of SRM can be found from previous relationships to achieve an accurate model, where the FEM results for flow attachment, inductance, and static torque are calculated and presented as a function of rotor position, current and permeability . Figures 3 and 4 display the properties of the SRM 12/8 over a single electrical cycle, namely inductance, flow contact, and constant torque.

We studied two cases of linear and nonlinear magnetic properties B = f (H). In linear situations, the wide current magnitude is not valid. It is also necessary to use the permeability is extracted from the magnetic properties B = f (H) in nonlinear cases to find out the true properties of the unit and to approximate the nonlinear case to the linear case.

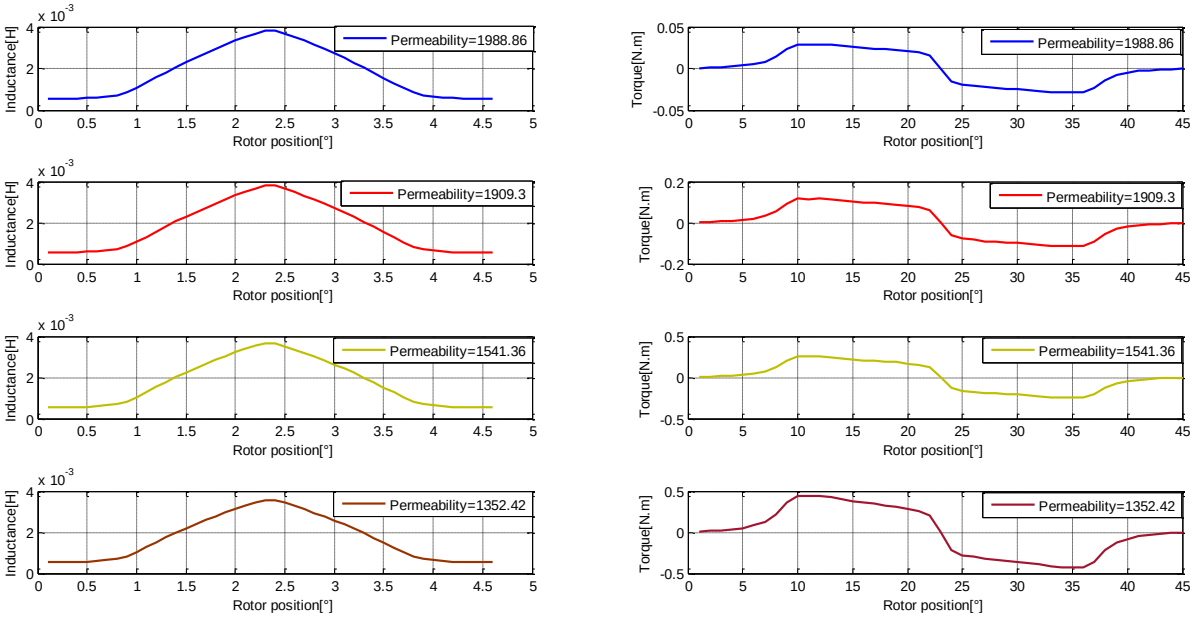

Fig. 5. Inductance and constant torque as a function of the rotating position and permeability of the linear case.

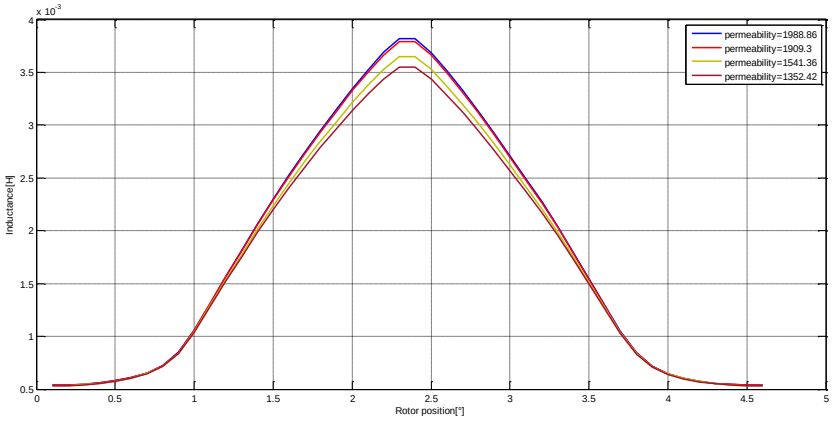

Fig. 6. Inductance characteristics as a function of the rotor position and permeability for linear case.

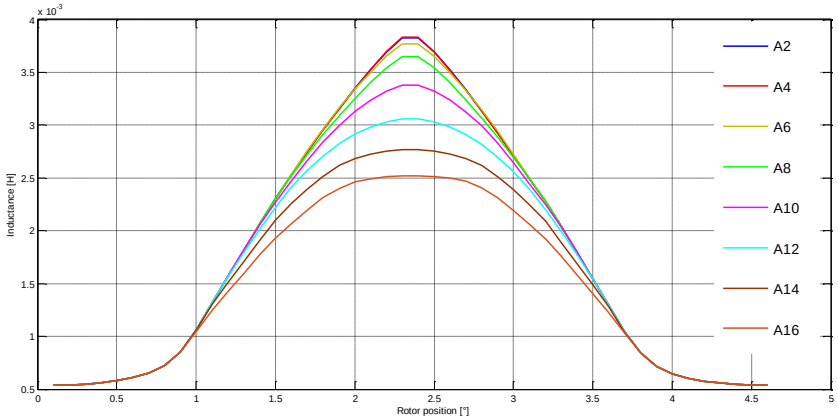

Fig. 7. Inductance characteristics as a function of the rotor position and the electrical current for nonlinear case.

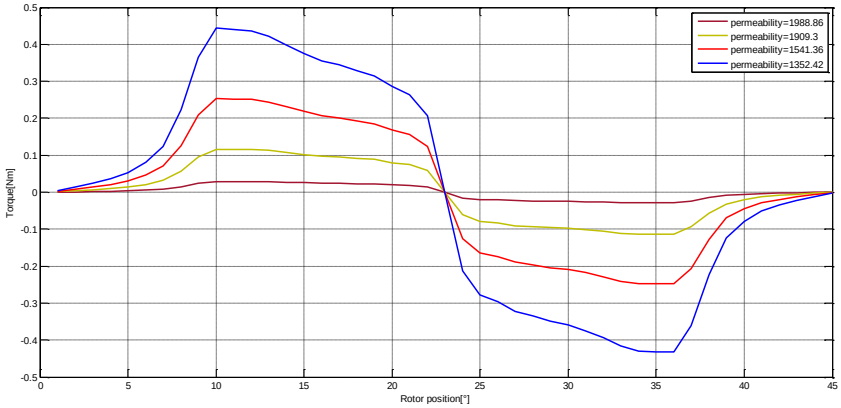

Fig. 8. Static torque as a function of the rotor position and permeability for linear case.

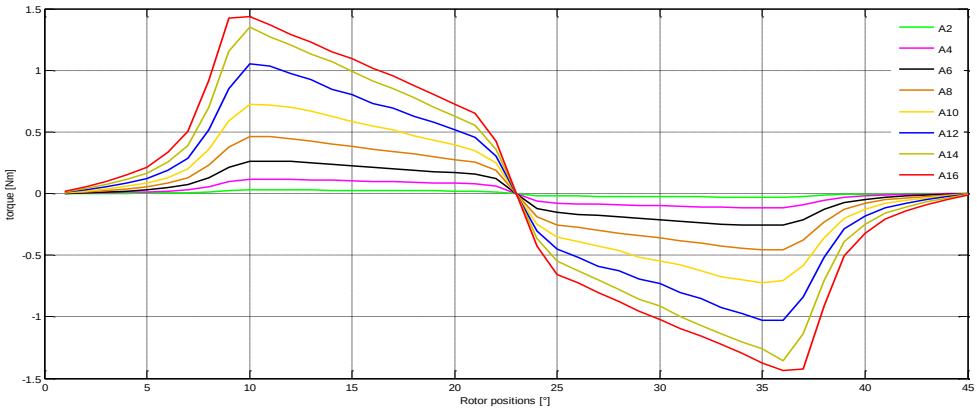

Fig. 9. Static torque as a function of the rotor position and the electrical current for non-linear case.

Inductance curve networks depend on the correlation between current and flow (Eq 4). It can be inferred from FEM modeling of the 12/8 SRM results that the two important factors influencing inductance variance are the specific position and magnetic saturation.

From Fig. 5, the inductance change and the constant torque are represented as a function of the position of rotation and the permeability of the linear state, the permeability values range from: permeability μ equal to 1352.42 to 1988.86. As shown in Fig.6, This is the inductance variance that varies only with the rotor position, because the inductance activity is highest at the rotor position, when the permeability values increase with increasing induction activity.

From Fig 7 and Fig 9, present the variation of inductance and constant torque in terms of position of rotation and case of nonlinear current, with permeability values ranging from: i = 2 A to 6 A. As shown in Fig.7, this is the variation of inductance only depending on the position the rotor, where the inductance activity is greater at the position of the linear rotor when the current values decrease with the increase in the inductance activity,

From Fig 6, Fig 7, Fig 8 and Fig 9, we note that the results are consistent with linear and nonlinear states, and that the values of inductance and torque:

- The permeability μ =1352.42 for the linear case with current i = 2A for the nonlinear case.

- The permeability μ =1541.36 for the linear state with current i = 4A for the nonlinear case.

- The permeability μ =1909.3 for the linear state with current i = 6A for the nonlinear case.

- The permeability μ =1988.86 for the linear state with current i = 8A for the nonlinear case.

These data show the effect of the difference in rotor position (air gap) and magnetic saturation, as in Fig 5, the result of inductance and static torque is proportional to the difference in rotor position and permeability in a linear condition. As in Fig 7 and fig.9, the result of inductance and static torque is proportional to the difference in the position of the rotor and the electric current in a nonlinear condition. Also, there is equalization in the results for the two cases by exploiting the permeability curve B=f(H) (see Figure1) using it in calculating the inductance and static torque of the linear case. In addition, the constant torque is proportional to the slope of the inductance curve, i.e. proportional to the derivative of inductance [11].

5. CONCLUSION

The study of the nonlinear and the approximate effects of the 12/8 SRM physical reality model using finite element method modeling has been explained in our study, in order to determine the magnetic properties of both cases.

The location of the SRM alignment in both cases was evident, when we considered the magnetic circuit saturation and gap distance variance. Moreover, when calculating the permeability from the curve B = f (H) used to calculate the magnetic property in a linear case, the increase in the permeability value corresponds to the increase in flux density. With rotational position change, the linear model of SRM was developed when we considered rotational position change (the difference in the air gap), and thus became a feature of SRM along with other behaviors.

After modeling and evaluating both cases, we conclude that FEM use of the SRM model has a significant effect, in order to provide more functionality and more engineering notes for more details on the behavior of the system. When designing the device or changing the control parameters, the SRM induction result is very sensitive, because it carries a nonlinear and approximate meaning of static or dynamic computational performance of a closer model of the coil.

In light of this work, we plan to research a smart and simple method that can approximate nonlinear features to linear one based on the permeability of the B=f (H) magnetization curve extractor.

6. References

[1] K.Vijayakumar, R. Karthikeyan et al., "Switched reluctance motor modeling, design, simulation, and analysis: a comprehensive review," IEEE Trans Magn, vol. 44, No. 12, pp. 4605 – 4617. 2008.

[2] C. Labiod, K. Srairi, B. Mahdad et al., "Optimum Performances for Non-linear Finite Elements Model of 8/6 Switched Reluctance Motor Based on Intelligent Routing Algorithms, " Advances In Electrical And Electronic Engineering (AEEE), Vol. 15, No. 1, pp. 1-10, 2017.

[3] Husain, I. and S. A. Hossain, "Modeling, simulation, and control of switched reluctance motor drives," IEEE Trans Ind Electron, vol. 52, No. 6, pp. 1625– 1635, 2005.11-[08]

[4] S. R. H. Hoole and P. R. P. Hoole, "Finite element programs forn teaching electromagnetics," IEEE Transaction in education, vol. E-29, 1986.

[5] G. E. Dawson, A. R. Eastham, and J. Mizia, "Switched reluctance motor torque characteristics: Finite element analysis and test results," IEEE Transaction in industrial applacations , vol. IA-23, No. 3, pp. 864–869, 1987.

[6] M. N. O. Sadiku, "A simple introduction to finite element analysis of electromagnetic problems," IEEE Transaction in education, vol. 32, No. 2, pp. 85-93,1989.

[7] C. Labiod, K. Srairi, B. Mahdad, M. E. H. Benbouzid, "A novel control technique for torque ripple minimization in switched reluctance motor through destructive interference, " Electrical Engineering, Vol. 100, pp. 481-490, 2017.

[8] B. Parreira, S. Rafael, A. J. Pires, and P. J. Costa Branco, "Obtaining the Magnetic Characteristics of an 8/6 Switched Reluctance Machine: From FEM
Analysis to the Experimental Tests," IEEE Transaction on industrial electronics, vol. 52, No. 6 pp. 1635-1643, 2005.

[9] X. Chen, J. Wu, "Calculation of inductances with 3-D FEM for SRM with segmental rotors and fully-picthed windings," 2014 17th International Conference on Electrical Machines and Systems (ICEMS), Hangzhou, China, pp. 1822-1824, 22-25 Oct 2014.

[10] M. Diko, P. Rafajdus and P. Makys, et al., "A Novel Concept of Short- Flux Path Switched Reluctance Motor for Electrical Vehicles," Advances in Electrical and Electronic Engineering, vol. 13, No. 3, pp. 206–2011, 2015.

[11] C. Labiod, et al., "Static and dynamic analysis of non-linear magnetic characteristics in switched reluctance motors based on circuit-coupled time stepping finite element method," Int J Syst Assur Eng Manag, Vol.8, Sup. 1, PP.47-55, 2017.

[12] C. Labiod, K. Srairi and B. Mahdad, et al., “Speed control of 8/6 switched reluctance motor with torque ripple reduction taking into account magnetic saturation effects,” Energy Proccedia, Vol. 74: pp.112– 121, 2015.
[13] J. Ye, B. Bilgin and A. Emadi, “An Extended-Speed Low-Ripple Torque Control of Switched Reluctance Motor Drives,” IEEE Transactions on Power Electronics, vol. 30, No. 3, pp. 1457 - 1470, 2015.